Bloom syndrome DNA helicase mitigates mismatch repair-dependent apoptosis

Yuka Uechi[1,2], Ryosuke Fujikane[1,3*], Sho Morita[1], Sachio Tamaoki[2], and Masumi Hidaka[1,3]

[1] Department of Physiological Sciences and Molecular Biology, Fukuoka Dental College, 2-15-1, Tamura, Sawaraku, Fukuoka, 814-0193, Japan

[2] Department of Oral Growth and Development, Fukuoka Dental College, 2-15-1, Tamura, Sawaraku, Fukuoka, 814-0193, Japan

[3] Oral Medicine Research Center, Fukuoka Dental College, 2-15-1, Tamura, Sawaraku, Fukuoka, 814-0193, Japan

*Corresponding author: Ryosuke Fujikane, email: fujikane@fdcnet.ac.jp

Abstract

Generation of O^6-methylguanine (O^6-meG) by DNA-alkylating agents such as N-methyl N-nitrosourea (MNU) activates the multiprotein mismatch repair (MMR) complex and the checkpoint response involving ATR/CHK1 and ATM/CHK2 kinases, which may in turn trigger cell cycle arrest and apoptosis. The Bloom syndrome DNA helicase BLM interacts with the MMR complex, suggesting functional relevance to repair and checkpoint responses. We observed a strong interaction of BLM with MMR proteins in HeLa cells upon treatment with MNU as evidenced by co-immunoprecipitation as well as colocalization in the nucleus as revealed by dual immunofluorescence staining. Knockout of BLM sensitized HeLa MR cells to MNU-induced cell cycle disruption and enhanced expression of the apoptosis markers cleaved caspase-9 and PARP1. MNU-treated BLM-deficient cells also exhibited a greater number of 53BP1 foci and greater phosphorylation levels of H2AX at S139 and RPA32 at S8, indicating the accumulation of DNA double-strand breaks. These findings suggest that BLM prevents double-strand DNA breaks during the MMR-dependent DNA damage response and mitigates O^6-meG-induced apoptosis.

Keywords

Mismatch repair, DNA damage response, cell cycle, apoptosis, alkylating agents

Introduction

Mismatch repair (MMR) is a highly conserved DNA repair system crucial for the removal of misincorporated nucleotides during DNA replication and the maintenance of genome integrity. The MMR also contributes to genome homeostasis by inducing apoptosis in response to the generation of O^6-methylguanine (O^6-meG) in DNA by alkylating agents such as N-methyl-N-

nitrosourea (MNU) and N-methyl-N-nitro-N-nitrosoguanidine [1,2]. O^6-methylguanine can pair with thymine and cytosine during DNA replication, resulting in O^6-meG/T mismatch and leading to G-to-A transition mutations, sister chromatid exchanges, and chromosomal aberrations [3]. The O^6-meG methyl group is removed primarily by methylguanine methyltransferase (MGMT) [4]; however, persistent O^6-meG/T pairing triggers recognition and binding by the multiprotein MMR complex, initiating DNA damage responses. This in turn activates the ATR/CHK1 and ATM/CHK2 axis checkpoints, which leads to mitochondria-associated apoptosis and elimination of cells harboring mutation-evoking base mismatches [5-7]. To understand the molecular mechanisms underlying O^6-meG-induced MMR-dependent apoptosis, our laboratory and others have investigated the interactions among MMR-related proteins and various DNA damage response and repair proteins upon alkylation [8-13]. Furthermore, MMR complex formation at O^6-meG/T mismatch sites triggers cell cycle arrest through the aforementioned DNA damage response, a process counteracted by homologous recombination (HR) [14-16]. To gain a more precise understanding of the regulatory mechanisms governing MMR, other DNA repair systems, and cell cycle checkpoint activity in response to alkylating agents, it is imperative to reveal the structural and functional relationships between MMR proteins and the multitude of other proteins found in the repair complex, referred to as the BRCA1-associated genome surveillance complex (BASC) [17].

The multifunctional BASC consists of the MMR proteins MutSα (a heterodimer of MSH2 and MSH6) and MutLα (a heterodimer of MLH1 and PMS2), and various other DNA repair proteins, including the RecQ family DNA helicase BLM. The activity of BLM is implicated in HR regulation and the resolution of arrested replication forks resulting from collisions with DNA secondary structures and nucleotide depletion. Loss-of-function mutations in BLM lead to Bloom syndrome, which is characterized by developmental defects and increased predisposition to various cancers at an early age. Cells lacking the BLM gene exhibit hypersensitivity to DNA-damaging agents and elevated sister chromatid exchange rates [18]. BLM forms a complex with TopoIIIα, RMI1, and RMI2 that facilitates resolution of Holliday junctions during HR-mediated double-strand break (DSB) repair [19]. In addition, BLM contributes to double-strand end resection by generating a long 3′ overhang single-strand DNA for invasion by the recombinase RAD51 [20,21]. Another function of BLM crucial for maintenance of genome integrity is the repair of stalled replication forks under replication stress. Specifically, BLM catalyzes replication fork regression, resulting in a chicken foot structure that supports DNA lesion bypass by template switching of DNA polymerase to restart the replication fork [22]. Furthermore, BLM helicase activity is essential for removing obstacles ahead of the replication fork, such as secondary structures and R-loops, particularly at the guanine-rich telomeric region, to ensure replication fork progression [23].

Thus, BLM is involved in the reparative response to both replication stress and subsequent DNA strand breaks.

Alkylating agents also induce MMR-dependent activation of ATR/CHK1 signaling [6,14], suggesting that the MMR complex may actually induce replication stress and that BLM functions to mitigate this effect as a part of the BASC. Although yeast two-hybrid studies have demonstrated an interaction between BLM and the MMR protein MLH1, BLM activity is not necessary for mismatch repair in human cell extracts [24,25]. Nonetheless, the interaction between BLM and the MMR complex suggests a potential cooperative function in regulating the response to alkylating agents. However, little direct functional relationship has been demonstrated.

In this study, we observed an augmented interaction between BLM and MMR factors in HeLa MR cells upon treatment with the DNA-alkylating agent MNU. Moreover, cells lacking BLM exhibited a greater apoptosis rate in response to MNU than wild-type cells. In addition, BLM-knockout cells demonstrated elevated production of DSBs as indicated by an increased number of 53BP1 foci and greater phosphorylation of H2AX and RPA32 following alkylation. Our findings imply that BLM is crucial for resolving replication perturbations induced by the MMR, thereby ensuring genome stability.

Materials and methods

Cell line and cultivation

HeLa MR cells were cultured as described previously [9]. For S phase synchronization, cells were cultured in medium containing 2.5 mM thymidine for 16 h, without thymidine for 8 h, and again in thymidine for 16 h. After washing with medium, cells were treated with the indicated concentrations of MNU.

Construction of the BLM-knockout cell

BLM-knockout (BLM-KO) cell lines were established using CRISPR/Cas9 (Addgene plasmid #62988) [26] as described previously [12] with the guide RNA sequence 5′-AGATTTCTTGCAGACTCCGA or GTTGGGTAGAGGTTCACTGA-3′. Cells lacking the BLM gene were then screened by immunoblotting using an anti-BLM antibody.

Gene knockdown

For targeted knockdown of MSH2 and MLH1, wild-type HeLa MR cells were transfected with MSH2-specific siRNA (5′-UAUAAUUCUUCCUUGUCCUUUCUCC-3′) or MLH1-specific siRNA (5′-UGCACAUUAACAUCCACAUUCUGGG-3′) according to the manufacturer’s instructions (Thermo Fisher).

Immunoblotting, Immunoprecipitation, and Immunofluorescent analysis

Immunoblotting, immunoprecipitation, and immunofluorescent analysis were performed as described previously [12] using the antibodies indicated in the figures. Immunoprecipitation of lysates from FLAG-tagged PMS2-expressing cells was also conducted as described [5]. The following primary antibodies were used for those assays: anti-ATM (#2773), anti-phospho-S1981 ATM (#13050), anti-BLM (#2742), anti-caspase-9 (#9502), anti-CHK1 (#2360), anti-phospho-S317 CHK1 (#12302), anti-CHK2 (#6334), anti-phospho-T68 CHK2 (#2661), anti-γH2AX (#7631), anti-phospho-S8 RPA32 (#54762), Cell Cycle Phase Determination Kit (#17498) (all from Cell Signaling Technology), anti-β-actin (010-27841, Fujifilm Wako), anti-phospho-T1989 ATR (GTX128145, GeneTex), anti-ATR (sc1887) and anti-lamin A/C (sc7292) (both from Santa Cruz Biotechnology), anti-MLH1 (554073), anti-PMS2 (556415), and anti-ORC2 (559670) (all from BD Biosciences), anti-FLAG M2 (F1804, Sigma), and anti-MSH2 (337900, Thermo Fisher Scientific). Alexa 488- and Alexa 568-conjugated anti-mouse and anti-rabbit antibodies for immunofluorescence staining were purchased from Thermo Fisher Scientific.

Flow cytometric analysis

Cells were treated with or without 25 μM MNU for 1 h as described previously [12] and cell cycle progression analyzed using a FACS Lyric flow cytometer (BD Biosciences).

Proximity ligation assay (PLA)

Twenty-four or 48 h after MNU treatment, HeLa MR cells were permeabilized with mCSK buffer containing 0.1% Triton X-100 for 5 min on ice, and then fixed with 4% paraformaldehyde for 10 min. The PLA was performed according to the manufacturer's instructions (Sigma) using anti-BLM and anti-MLH1 antibodies. PLA signals were visualized by confocal laser scanning microscopy (LSM-710; Zeiss).

Statistics

The statistically significant differences of multiple values were determined by one-way ANOVA with Turkey's multiple comparison test using Prism9 (GraphPad Software), and those of two values were determined by unpaired Student's t test.

Results

Treatment of HeLa MR cells with a DNA-alkylating agent enhances the association

between BLM and MMR complex proteins

Within the BASC, BLM interacts directly with the MMR proteins MSH2/MSH6 and MLH1 [17,25,27] but is dispensable for MMR in vitro [24], so the functional significance of this interaction remains unclear. We speculated that a functional interaction relevant to MMR would be modulated by DNA alkylation, and so compared the co-immunoprecipitation (co-IP) of MMR proteins with BLM in chromatin-enriched fractions from untreated and MNU-treated HeLa MR cells deficient in MGMT (and thus prone to O^6-methylguanine accumulation). An immobilized anti-BLM antibody immunoprecipitated MutLα (MLH1/PMS2) and MutSα (MSH2/MSH6) from the chromatin fractions of both untreated (0 h) and MNU-treated cells (Figure 1a). However, the interaction was substantially stronger after 24 h of MNU treatment. This MNU-dependent interaction was further confirmed by reciprocal immunoprecipitation using an anti-FLAG antibody and chromatin fractions from cells expressing FLAG-tagged PMS2 (Figure 1b). In addition, immunofluorescence staining of fixed HeLa MR cells revealed that MNU treatment increased the number of nuclear foci containing colocalized BLM and MLH1 (Figure 1c, d). This MNU-dependent association was further confirmed by a PLA (Figure 1e). These results strongly suggest that BLM is recruited to sites of MNU-induced DNA damage through interactions with MMR proteins MLH1 and MSH2.

Depletion of BLM sensitizes HeLa MR cells to MNU

To investigate BLM functions in the cellular response to alkylation, we generated two independent BLM-knockout HeLa MR cell (BLM-KO) lines using the CRISPR/Cas9 method [26] and examined differences in MNU sensitivity with wild-type cells. Immunoblotting confirmed the absence of BLM expression in BLM-KO cells, while the expression levels of MSH2 and MLH1 genes were unaffected (Figure 2a). Both BLM-KO lines were more sensitive to MNU-induced cell death than wild-type cells as evidenced by colony counting assays (Figure 2b). This enhanced MNU sensitivity was mitigated by expression of exogenous BLM (Figure 2c, d), indicating that BLM is required for recovery from MNU-induced DNA damage. In addition, this enhanced sensitivity of BLM-KO cells to MNU was abrogated by siRNA-induced knockdown of MLH1 and MSH2 (Figure 2e, f).

Depletion of BLM in HeLa MR cells enhances MNU-induced DNA damage, cell cycle arrest, and apoptotic signaling

To directly examine the effects of BLM knockout on cell cycle progression, DNA damage, and apoptosis, wild-type HeLa MR cells and BLM-KO cells were synchronized in S phase using a double thymidine block protocol, treated with or without MNU, returned to normal medium, and analyzed by flow cytometry (Figure 3a, S1a) and immunoblotting (Figure 3b, c, d, S1b).

Without MNU treatment, both wild-type and BLM-deficient cell lines showed almost the same cell cycle progressions after release from synchronization as were evident by flow cytometric profiles and immunoblotting patterns of cell cycle indicators (Figure S1). When cells were treated with MNU, while wild-type HeLa MR cells smoothly transitioned from S phase to G2/M and G1, cells exhibited a markedly prolonged S phase and modest G2 arrest from 18 to 36 h after onset of MNU exposure. However, these cells then began to recover from G2 arrest and progressed to G1 and S phase. In contrast, BLM-KO cells exhibited significantly slower progression to the second S phase and a protracted second G2 phase, characterized by elevated levels of CDT1 and phospho-H3, starting 48 h after MNU treatment (Figure 3b). In addition, there was a gradual increase in the population of sub-G1 cells, indicating the induction of apoptosis and consistent with the greater MNU sensitivity in colony counting assays (Figure 2b).

To examine the influence of BLM deficiency on the DNA damage response, we conducted immunoblotting using antibodies against checkpoint kinases and apoptosis markers. BLM-KO cells demonstrated significantly greater phosphorylation of ATR and CHK1 beginning 18 h after the onset of MNU treatment compared to similarly treated wild-type cells (Figure 3c), and this elevated checkpoint protein phosphorylation (activation) persisted until cells became apoptotic as evidenced by enhanced cleavage of caspase-9 and PARP-1 (Figure 3d). Furthermore, concurrent ATM/CHK2 phosphorylation was observed primarily from 24 to 60 h after MNU exposure, which corresponded to the time of G2 arrest and accumulation of the subG1 population (Figure 3a) observed by flow cytometry. These results suggest that in the absence of BLM, replication stress induced by MNU may lead to enhanced DSB generation, cell cycle arrest, and apoptosis.

Generation of DSBs in BLM-KO cells after MNU treatment

To provide further evidence that BLM contributes to the DNA damage response, we conducted immunoblotting assays of the chromatin fractions from synchronized wild-type and BLM-KO cells using antibodies against BLM, MMR proteins, and DSB marker proteins (Figure 4). The MMR protein MLH1 was loaded on the damaged chromatin throughout the cell cycle in both wild-type and BLM-KO cells. However, there was a substantial decrease in MLH1 loading concomitant with MNU-induced apoptosis of BLM-KO cells. In wild-type cells, BLM levels on chromatin increased gradually from 18 to 36 h in MNU, coinciding with entry into the second S and G2 phases. This observation suggests that BLM contributes to the mitigation of replication stress induced by MNU.

To confirm the formation of DSBs and the reparative function of BLM, we measured the phosphorylation levels of RPA32 at serine 8 and H2AX at serine 139 by immunoblotting

and conducted immunostaining for 53BP1 as a DBS marker (Figure 4, S2). As illustrated in Figure 4a, RPA32 phosphorylation became evident 18 to 48 h preceding the MNU-induced apoptosis events shown in Figure 3d, suggesting activation of DNA-PKcs in response to DSBs. The kinetics of H2AX and RPA32 phosphorylation were also similar, indicating the active involvement of ATM or ATR checkpoint kinases. In addition, the number of 53BP1 foci was significantly greater in BLM-KO cells than wild-type cells starting 24 h after the initiation of MNU treatment (Figure 4b). The elevation of 53BP1 foci was completely abolished by depletion of MMR genes (Figure S3), relevant to MMR-dependent sensitivity of BLM-KO cells (Figure 2f). Collectively, these findings suggest that BLM protects cells from apoptosis by preventing the formation of DSBs due to MMR-dependent replication stress during the second S phase.

Discussion

A constitutive direct interaction of BLM with MLH1 has been demonstrated in vitro using recombinant proteins and the yeast two-hybrid system [24,25]. We also observed an increased association between BLM and MLH1 in the presence of a DNA-alkylating agent (Figure 1), suggesting that the MMR complex may recruit BLM to sites of DNA damage. However, BLM is not necessary for MMR [24,28], and there are conflicting reports on whether the MMR complex stimulates BLM helicase activity [27,28]. In this notion, our results support the perspective that BLM is involved in the process following MMR-dependent reaction, rather than MMR-mediated futile repair per se. Subsequent experiments demonstrated that BLM promotes cell survival by mitigating DNA replication stress associated with the MMR.

Activation of the ATR/CHK1 and ATM/CHK2 axis checkpoints are indicative of DNA replication stress and DSB formation, respectively [29,30], and both ATR/CHK1 and ATM/CHK2 pathways were sequentially activated by DNA alkylation (Figure 3), in accord with previous studies [6,8,14]. Thus, elevated ATM/CHK2 activation in BLM-KO cells during MNU treatment may have resulted from the accumulation of DSBs (Figures 3 and 4). It has been proposed that mismatches formed by deoxythymidine incorporated in opposition to O^6-meG on the template strand cause a futile MMR cycle and leave ssDNA regions, which may cause DSBs upon formation of the next round-DNA replication fork [14]. The current findings suggest that BLM may protect replication forks from collapse and/or enhance the HR process for DSB repair after MNU treatment. Indeed, BLM can eliminate stalled replication forks by providing an alternative template using a nascent DNA strand for replication, resulting in the formation of a chicken foot structure that bypasses the DNA lesion [22]. Therefore, our observations showing retardation of the second S phase followed by G2 arrest in BLM-KO cells during MNU treatment may be related to the inability of BLM-deficient cells to mitigate

replication stress caused by MMR-mediated actions on chromatin containing O^6-meG.

The HR pathway is crucial for survival against MMR-dependent insults in DNA triggered by O^6-meG, and cells surviving exposure to alkylating agents carry chromosomes with an elevated signature of sister chromatid exchange [14]. The BLM helicase contributes to HR by facilitating resolution of Holliday junctions and end resection of DSBs [20,21]. Furthermore, in vitro studies using purified MMR proteins have indicated that MutSα stimulates the branch migration activity of BLM and other RecQ helicases such as RECQ1 and WRN [27,31,32]. Hence, the elevated sensitivity of BLM-KO cells to MNU may result from a defect in HR that causes DSB accumulation and ultimately leads to apoptotic cell death.

A BLM deficiency in humans causes Bloom syndrome, and cells from Bloom syndrome patients show hypersensitivity to several DNA-damaging agents [23]. In contrast, genome analysis has demonstrated elevated BLM expression in multiple cancer types [33]. Given the multifunctional role of BLM in DNA repair systems, this elevated expression is likely to impact the sensitivity to genotoxic anticancer drugs. Consequently, BLM has emerged as a promising therapeutic target for cancer treatment. Our findings support the potential of BLM inhibitors for cancer treatment, particularly when used in conjunction with alkylating agents.

Acknowledgments

The authors thank Dr. Yoshimichi Nakatsu for helpful discussion. This work was supported by Promotion and Mutual Aid Corporation for Private Schools of Japan, JSPS KAKENHI, Grant Number 22K09956 (to R.F.) and Grant Number 20K09915 (to M.H.).

Author contribution

Yuka Uechi: Investigation, Writing - Original Draft, Visualization Ryosuke Fujikane: Conceptualization, Investigation, Validation, Formal analysis, Resources, Writing - Original Draft, Writing - Review & Editing, Funding acquisition Sho Morita: Resources Sachio Tamaoki: Supervision Masumi Hidaka: Conceptualization, Validation, Writing - Original Draft, Writing - Review & Editing, Project administration, Funding acquisition.

Ethics approval

Not applicable

Competing interests

The authors declare no competing interests.

Figure legends

Figure 1. Treatment with the DNA-alkylating agent MNU increases the interaction of BLM with mismatch repair (MMR) complex proteins in HeLa MR cells. (a) Immunoprecipitation experiment showing enhanced interactions of BLM with MMR proteins MutSα and MutLα after MNU exposure. The chromatin-enriched fraction (input) was prepared from HeLa MR cells at the indicated times after treatment with 1 mM MNU. Beads conjugated to anti-BLM were incubated with this fraction and precipitates separated by SDS-PAGE, followed by immunoblotting with antibodies against MSH2, MSH6, MLH1, PMS2, and origin recognition complex 2 (ORC2). IgG was used as a control. The asterisk indicates non-specific bands. (b) Immunoprecipitation experiments using HeLa MR cells expressing Flag-tagged PMS2 treated with 25 μM MNU. The assay with anti-FLAG antibody was performed as in (a). (c) Immunofluorescence staining of HeLa MR cells for BLM (red) and MLH1 (green) showing progressively enhanced colocalization at 24 and 48 h after 1 mM MNU treatment. Nuclei were counterstained with DAPI (blue). (d) Percentage of MLH1 foci colocalized with BLM, determined by counting the foci in (c). **: $p<0.01$, ***: $p<0.001$. (e) Analysis of the BLM-MLH1 interaction by proximity ligation assay conducted on HeLa MR cells at the indicated times after treatment with 25 μM MNU.

Figure 2. BLM-knockout increases the sensitivity of HeLa MR cells to MNU in an MMR-dependent manner. (a) Whole-cell extracts prepared from wild-type HeLa MR cells and BLM-knockout (KO) cells were immunoblotted for BLM, MSH2, MLH1, and β-actin (as a loading control) to confirm KO. (b) BLM knockout enhanced MNU sensitivity. Wild-type HeLa MR and BLM-KO cells were treated with the indicated MNU concentration, and the numbers of colonies were counted. Results are presented as the mean survival fraction (with standard error) from three independent experiments. (c) Immunoblotting of whole-cell extracts prepared from HeLa MR cells, BLM-KO#2 cells, and BLM-KO#2 cells transfected with an exogenous BLM vector to confirm the protein levels of BLM, respectively. (d) Restoration of BLM expression mitigated the enhanced MNU sensitivity. The survival fractions of HeLa MR, BLM-KO#2, and BLM-expressing BLM-KO#2 cells are shown as in (b). (e) The protein levels of BLM, MSH2, and MLH1 3 days after transfection of wild-type and BLM-KO cells with siRNAs targeting MSH2 and MLH1 as determined by immunoblotting to confirm knockdown efficacy. (f) The enhanced sensitivity of BLM-KO cells to MNU was dependent on MMR function as knockdown of MSH2 and MLH canceled the sensitivity. Cells were treated as in (b). *: $p<0.05$, ****: $p<0.0001$

Figure 3. Knockout of BLM enhanced the MNU-induced DNA damage response during cell cycle progression. HeLa MR and BLM-KO cells were synchronized in early S phase and released after treatment with 25 μM MNU. (a) Cell cycle phase distributions of wild-type HeLa MR cells (upper panels) and BLM-KO cells (lower panels) after MNU treatment revealed by flow cytometry. (b - d) Whole-cell extracts prepared from cells were subjected to SDS-PAGE, followed by immunoblotting using antibodies against cell cycle indicators (b), checkpoint proteins (c), apoptosis marker proteins (d), and β-actin (the loading control).

Figure 4. Knockout of BLM enhances accumulation of DNA double-strand breaks (DSBs). (a) Chromatin fractions prepared from HeLa MR and BLM-KO cells were subjected to SDS-PAGE, followed by immunoblotting for MMR proteins, DSB markers, and lamin as the loading control. (b) Immunostaining for 53BP1 foci in HeLa MR and BLM-KO cells at the indicated times after MNU exposure. Foci were counted using ImageJ. ****: $p<0.0001$, *: $p<0.05$, ns: not significance.

References

[1] B. Kaina, A. Ziouta, K. Ochs, T. Coquerelle, Chromosomal instability, reproductive cell death and apoptosis induced by O6-methylguanine in Mex-, Mex+ and methylation-tolerant mismatch repair compromised cells: facts and models, Mutation research 381 (1997) 227-241. 10.1016/s0027-5107(97)00187-5.

[2] P. Karran, P. Macpherson, S. Ceccotti, E. Dogliotti, S. Griffin, M. Bignami, O6-methylguanine residues elicit DNA repair synthesis by human cell extracts, The Journal of biological chemistry 268 (1993) 15878-15886.

[3] B. Kaina, O. Aurich, Dependency of the yield of sister-chromatid exchanges induced by alkylating agents on fixation time. Possible involvement of secondary lesions in sister-chromatid exchange induction, Mutation research 149 (1985) 451-461. 10.1016/0027-5107(85)90163-0.

[4] Y. Tominaga, T. Tsuzuki, A. Shiraishi, H. Kawate, M. Sekiguchi, Alkylation-induced apoptosis of embryonic stem cells in which the gene for DNA-repair, methyltransferase, had been disrupted by gene targeting, Carcinogenesis 18 (1997) 889-896.

[5] M. Hidaka, Y. Takagi, T.Y. Takano, M. Sekiguchi, PCNA-MutSalpha-mediated binding of MutLalpha to replicative DNA with mismatched bases to induce apoptosis in human cells, Nucleic Acids Res 33 (2005) 5703-5712. 10.1093/nar/gki878.

[6] L. Stojic, N. Mojas, P. Cejka, M. Di Pietro, S. Ferrari, G. Marra, J. Jiricny, Mismatch repair-dependent G2 checkpoint induced by low doses of SN1 type methylating agents requires the ATR kinase, Genes & development 18 (2004) 1331-1344. 10.1101/gad.294404.

[7] W.P. Roos, B. Kaina, DNA damage-induced cell death by apoptosis, Trends in molecular medicine 12 (2006) 440-450. 10.1016/j.molmed.2006.07.007.
[8] R. Fujikane, K. Komori, M. Sekiguchi, M. Hidaka, Function of high-mobility group A proteins in the DNA damage signaling for the induction of apoptosis, Scientific reports 6 (2016) 31714. 10.1038/srep31714.
[9] R. Fujikane, M. Sanada, M. Sekiguchi, M. Hidaka, The identification of a novel gene, MAPO2, that is involved in the induction of apoptosis triggered by O(6)-methylguanine, PloS one 7 (2012) e44817. 10.1371/journal.pone.0044817.
[10] D. Gupta, C.D. Heinen, The mismatch repair-dependent DNA damage response: Mechanisms and implications, DNA Repair (Amst) 78 (2019) 60-69. 10.1016/j.dnarep.2019.03.009.
[11] K.D. Brown, A. Rathi, R. Kamath, D.I. Beardsley, Q. Zhan, J.L. Mannino, R. Baskaran, The mismatch repair system is required for S-phase checkpoint activation, Nature genetics 33 (2003) 80-84. 10.1038/ng1052.
[12] M. Rikitake, R. Fujikane, Y. Obayashi, K. Oka, M. Ozaki, M. Hidaka, MLH1-mediated recruitment of FAN1 to chromatin for the induction of apoptosis triggered by O(6) -methylguanine, Genes to cells : devoted to molecular & cellular mechanisms 25 (2020) 175-186. 10.1111/gtc.12748.
[13] Y. Takeishi, R. Fujikane, M. Rikitake, Y. Obayashi, M. Sekiguchi, M. Hidaka, SMARCAD1-mediated recruitment of the DNA mismatch repair protein MutLalpha to MutSalpha on damaged chromatin induces apoptosis in human cells, The Journal of biological chemistry 295 (2020) 1056-1065. 10.1074/jbc.RA119.008854.
[14] N. Mojas, M. Lopes, J. Jiricny, Mismatch repair-dependent processing of methylation damage gives rise to persistent single-stranded gaps in newly replicated DNA, Genes & development 21 (2007) 3342-3355. 10.1101/gad.455407.
[15] P. Cejka, N. Mojas, L. Gillet, P. Schar, J. Jiricny, Homologous recombination rescues mismatch-repair-dependent cytotoxicity of S(N)1-type methylating agents in S. cerevisiae, Current biology : CB 15 (2005) 1395-1400. 10.1016/j.cub.2005.07.032.
[16] S. Quiros, W.P. Roos, B. Kaina, Rad51 and BRCA2--New molecular targets for sensitizing glioma cells to alkylating anticancer drugs, PloS one 6 (2011) e27183. 10.1371/journal.pone.0027183.
[17] Y. Wang, D. Cortez, P. Yazdi, N. Neff, S. Elledge, J. Qin, BASC, a super complex of BRCA1-associated proteins involved in the recognition and repair of aberrant DNA structures, Genes & development 14 (2000) 927-939.
[18] J. German, Bloom syndrome: a mendelian prototype of somatic mutational disease, Medicine 72 (1993) 393-406.

[19] L. Wu, I. Hickson, The Bloom's syndrome helicase suppresses crossing over during homologous recombination, Nature 426 (2003) 870-874.
[20] J.M. Daley, T. Chiba, X. Xue, H. Niu, P. Sung, Multifaceted role of the Topo IIIalpha-RMI1-RMI2 complex and DNA2 in the BLM-dependent pathway of DNA break end resection, Nucleic Acids Res 42 (2014) 11083-11091. 10.1093/nar/gku803.
[21] A. Sturzenegger, K. Burdova, R. Kanagaraj, M. Levikova, C. Pinto, P. Cejka, P. Janscak, DNA2 cooperates with the WRN and BLM RecQ helicases to mediate long-range DNA end resection in human cells, The Journal of biological chemistry 289 (2014) 27314-27326. 10.1074/jbc.M114.578823.
[22] C. Ralf, I.D. Hickson, L. Wu, The Bloom's syndrome helicase can promote the regression of a model replication fork, The Journal of biological chemistry 281 (2006) 22839-22846. 10.1074/jbc.M604268200.
[23] L. Wu, I. Hickson, RecQ helicases and cellular responses to DNA damage, Mutation research 509 (2002) 35-47.
[24] G. Langland, J. Kordich, J. Creaney, K.H. Goss, K. Lillard-Wetherell, K. Bebenek, T.A. Kunkel, J. Groden, The Bloom's syndrome protein (BLM) interacts with MLH1 but is not required for DNA mismatch repair, The Journal of biological chemistry 276 (2001) 30031-30035. 10.1074/jbc.M009664200.
[25] G. Pedrazzi, C. Perrera, H. Blaser, P. Kuster, G. Marra, S.L. Davies, G.H. Ryu, R. Freire, I.D. Hickson, J. Jiricny, I. Stagljar, Direct association of Bloom's syndrome gene product with the human mismatch repair protein MLH1, Nucleic Acids Res 29 (2001) 4378-4386.
[26] F.A. Ran, P.D. Hsu, J. Wright, V. Agarwala, D.A. Scott, F. Zhang, Genome engineering using the CRISPR-Cas9 system, Nature protocols 8 (2013) 2281-2308. 10.1038/nprot.2013.143.
[27] Q. Yang, R. Zhang, X.W. Wang, S.P. Linke, S. Sengupta, I.D. Hickson, G. Pedrazzi, C. Perrera, I. Stagljar, S.J. Littman, P. Modrich, C.C. Harris, The mismatch DNA repair heterodimer, hMSH2/6, regulates BLM helicase, Oncogene 23 (2004) 3749-3756. 10.1038/sj.onc.1207462.
[28] G. Pedrazzi, C.Z. Bachrati, N. Selak, I. Studer, M. Petkovic, I.D. Hickson, J. Jiricny, I. Stagljar, The Bloom's syndrome helicase interacts directly with the human DNA mismatch repair protein hMSH6, Biol Chem 384 (2003) 1155-1164. 10.1515/BC.2003.128.
[29] K.S. Keegan, D.A. Holtzman, A.W. Plug, E.R. Christenson, E.E. Brainerd, G. Flaggs, N.J. Bentley, E.M. Taylor, M.S. Meyn, S.B. Moss, A.M. Carr, T. Ashley, M.F. Hoekstra, The Atr and Atm protein kinases associate with different sites along meiotically pairing chromosomes, Genes & development 10 (1996) 2423-2437. 10.1101/gad.10.19.2423.
[30] A. Ciccia, S.J. Elledge, The DNA damage response: making it safe to play with knives, Mol Cell 40 (2010) 179-204. 10.1016/j.molcel.2010.09.019.
[31] K.M. Doherty, S. Sharma, L.A. Uzdilla, T.M. Wilson, S. Cui, A. Vindigni, R.M. Brosh, Jr.,

RECQ1 helicase interacts with human mismatch repair factors that regulate genetic recombination, The Journal of biological chemistry 280 (2005) 28085-28094. 10.1074/jbc.M500265200.
[32] N. Saydam, R. Kanagaraj, T. Dietschy, P.L. Garcia, J. Pena-Diaz, I. Shevelev, I. Stagljar, P. Janscak, Physical and functional interactions between Werner syndrome helicase and mismatch-repair initiation factors, Nucleic Acids Res 35 (2007) 5706-5716. 10.1093/nar/gkm500.
[33] E. Kaur, R. Agrawal, S. Sengupta, Functions of BLM Helicase in Cells: Is It Acting Like a Double-Edged Sword?, Frontiers in genetics 12 (2021) 634789. 10.3389/fgene.2021.634789.

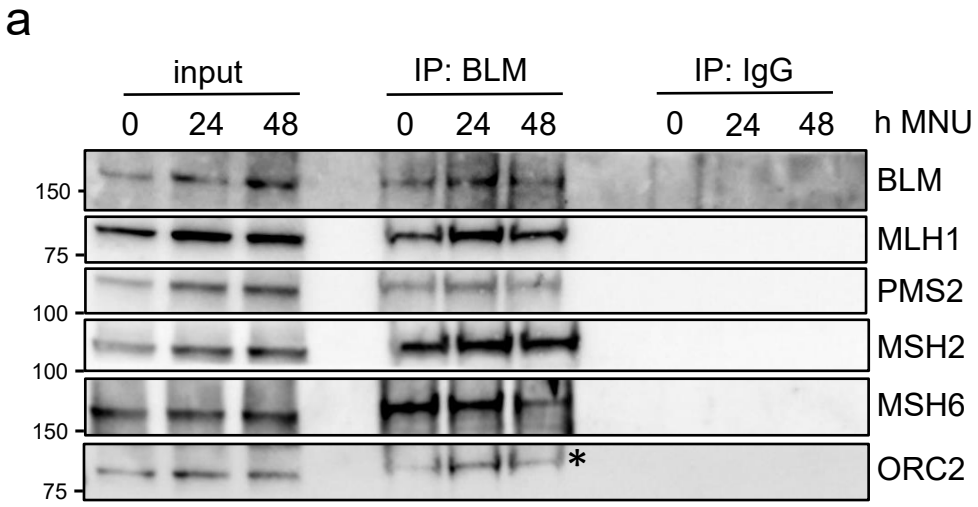
a
input
IP: BLM
IP: IgG
0 24 48 0 24 48 0 24 48 h MNU
150
75
100
100
150
75
BLM
MLH1
PMS2
MSH2
MSH6
ORC2
*

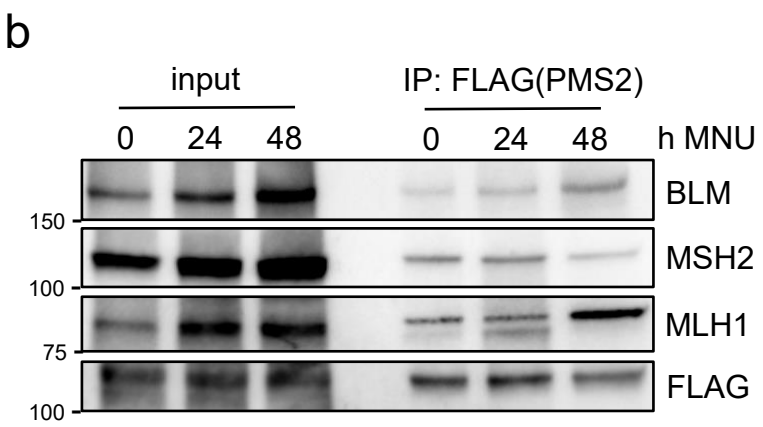
b
input
IP: FLAG(PMS2)
0 24 48 0 24 48 h MNU
150
100
75
100
BLM
MSH2
MLH1
FLAG

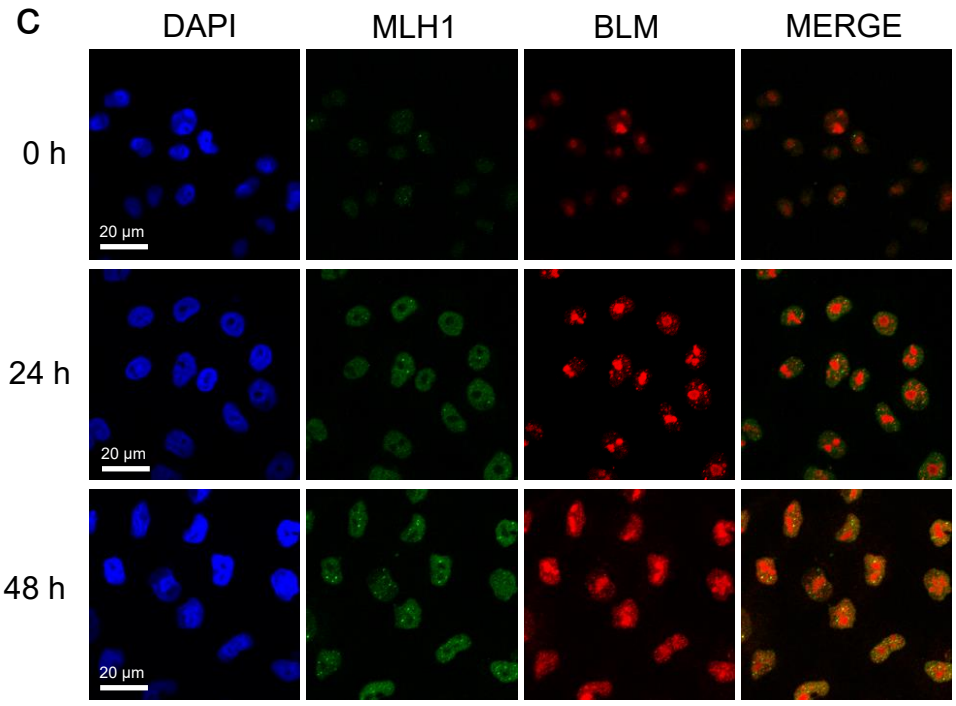
c
DAPI
MLH1
BLM
MERGE
0 h
24 h
48 h
20 µm

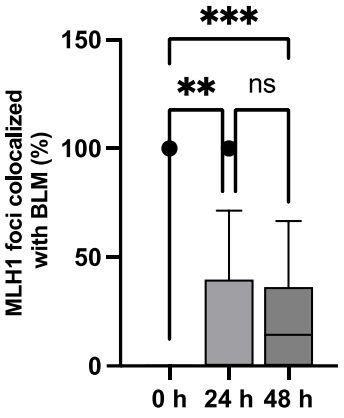
d
***
**
ns
150
100
50
0
MLH1 foci colocalized with BLM (%)
0 h 24 h 48 h

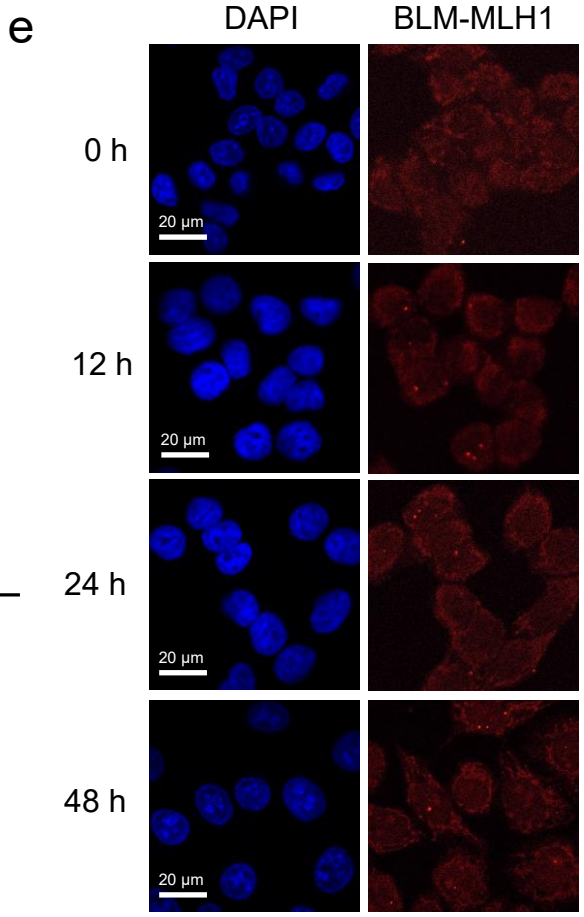
e
DAPI
BLM-MLH1
0 h
12 h
24 h
48 h
20 µm

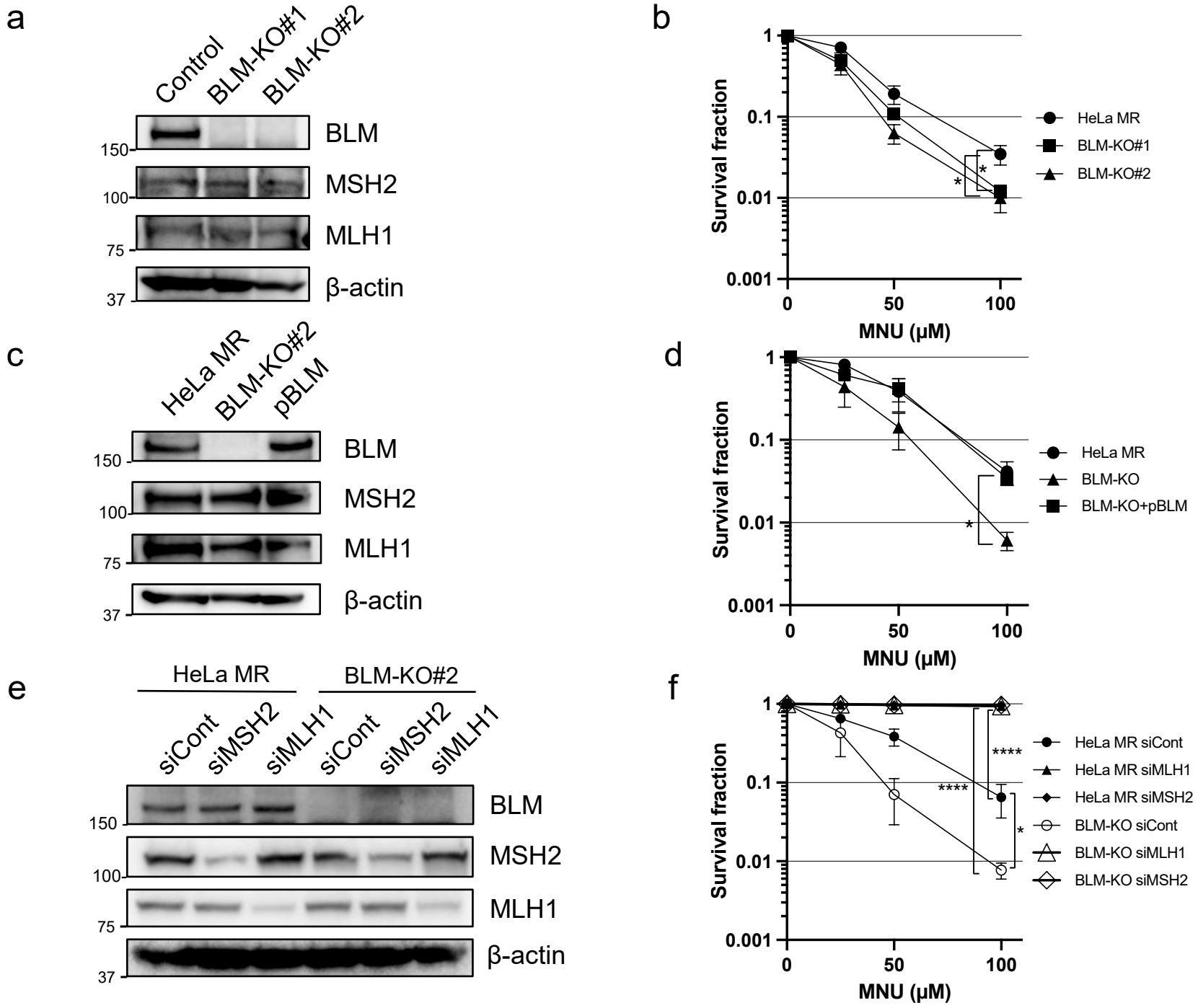
a
Control
BLM-KO#1
BLM-KO#2
150
100
75
37
BLM
MSH2
MLH1
β-actin
b
Survival fraction
1
0.1
0.01
0.001
0
50
100
MNU (μM)
HeLa MR
BLM-KO#1
BLM-KO#2
*
*
c
HeLa MR
BLM-KO#2
pBLM
150
100
75
37
BLM
MSH2
MLH1
β-actin
d
Survival fraction
1
0.1
0.01
0.001
0
50
100
MNU (μM)
HeLa MR
BLM-KO
BLM-KO+pBLM
*
e
HeLa MR
BLM-KO#2
siCont
siMSH2
siMLH1
siCont
siMSH2
siMLH1
150
100
75
37
BLM
MSH2
MLH1
β-actin
f
Survival fraction
1
0.1
0.01
0.001
0
50
100
MNU (μM)
HeLa MR siCont
HeLa MR siMLH1
HeLa MR siMSH2
BLM-KO siCont
BLM-KO siMLH1
BLM-KO siMSH2
****
****
*

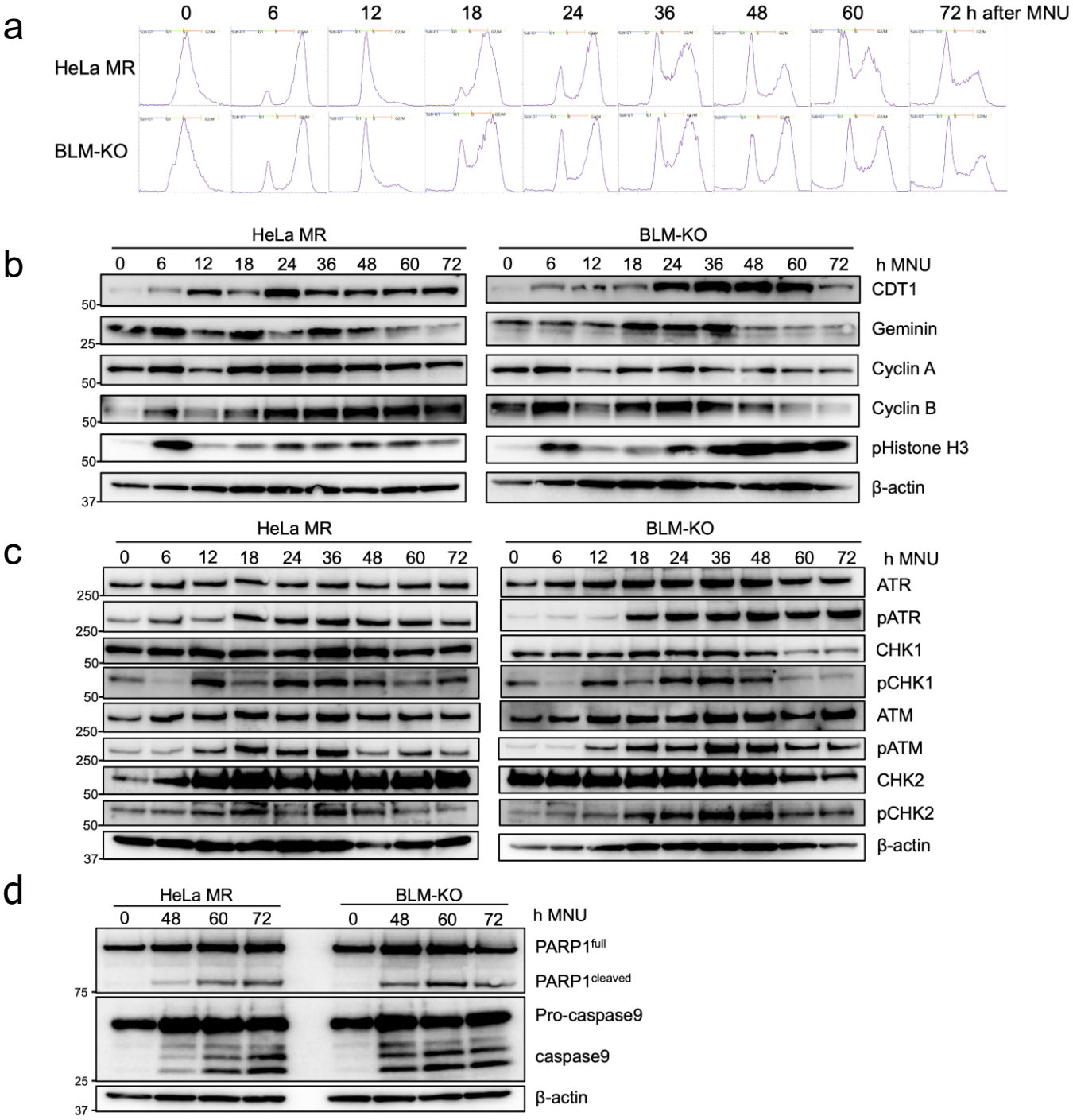
a
0
6
12
18
24
36
48
60
72 h after MNU
HeLa MR
BLM-KO
b
HeLa MR
BLM-KO
0 6 12 18 24 36 48 60 72
h MNU
CDT1
Geminin
Cyclin A
Cyclin B
pHistone H3
β-actin
50
25
50
50
50
37
c
HeLa MR
BLM-KO
0 6 12 18 24 36 48 60 72
h MNU
ATR
pATR
CHK1
pCHK1
ATM
pATM
CHK2
pCHK2
β-actin
250
250
50
50
250
250
50
50
37
d
HeLa MR
BLM-KO
0 48 60 72
h MNU
PARP1full
PARP1cleaved
Pro-caspase9
caspase9
β-actin
75
25
37

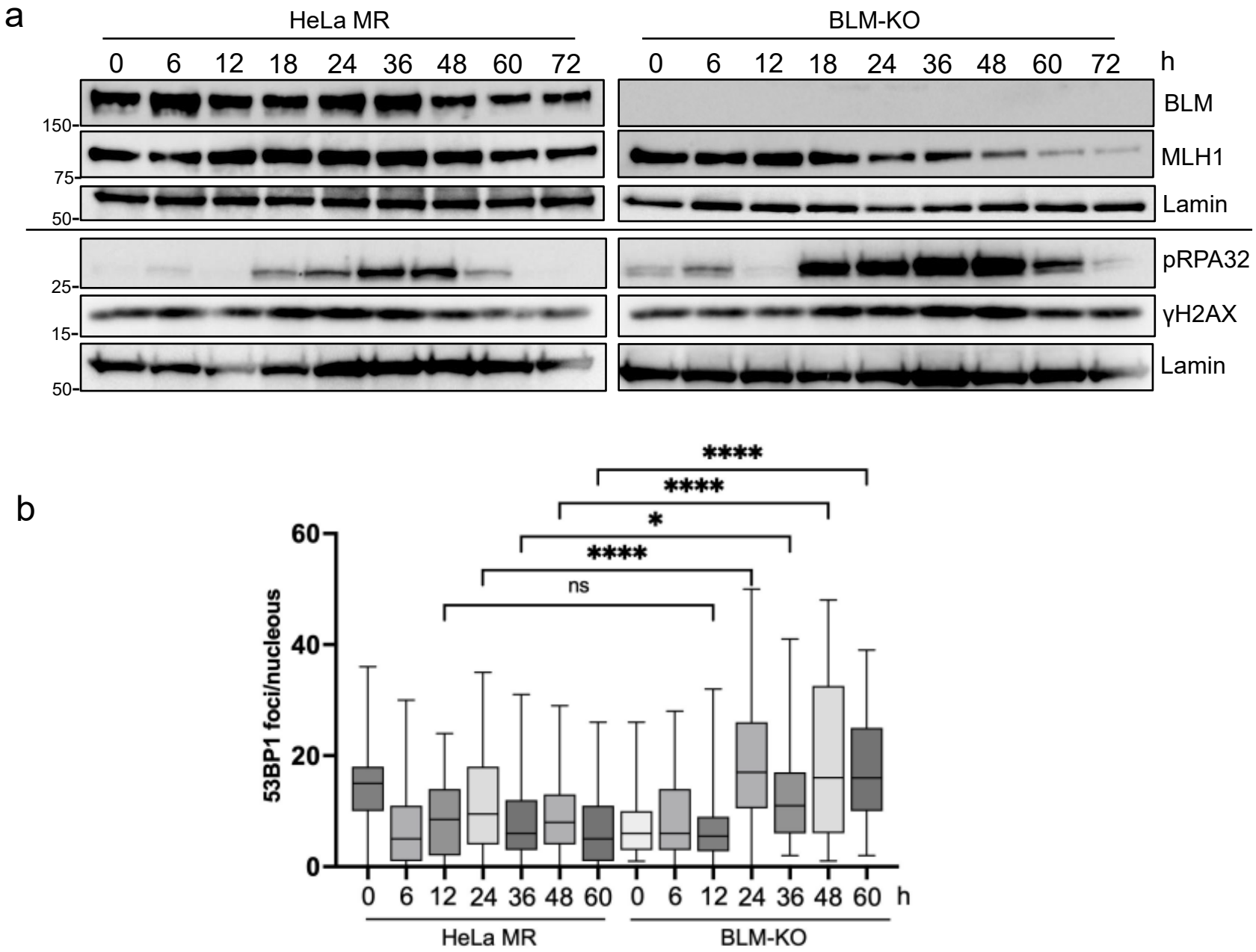
a
HeLa MR
BLM-KO
0 6 12 18 24 36 48 60 72
h
BLM
MLH1
Lamin
pRPA32
γH2AX
Lamin
150
75
50
25
15
50
b
53BP1 foci/nucleous
60
40
20
0
****
****
*
****
ns
0 6 12 24 36 48 60 0 6 12 24 36 48 60 h
HeLa MR
BLM-KO

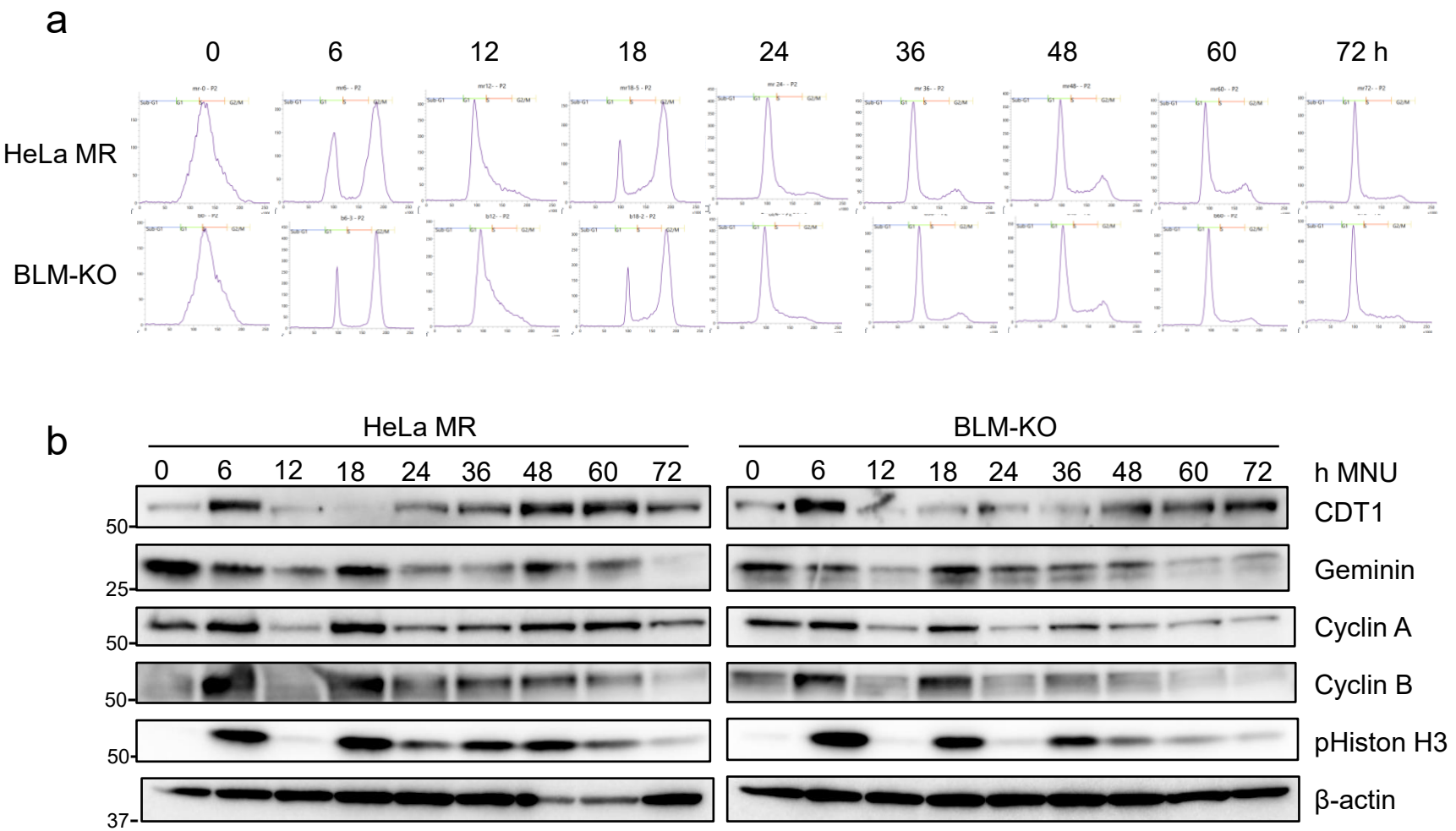

Figure S1 Cell cycle profiles of HeLa MR cells and BLM-KO cells. Cells were synchronized in early S-phase and then released in normal medium without MNU treatment. (a) Cell cycle phase distribution of HeLa MR (upper panels) and BLM-KO (lower panels) determined by flow cytometry. (b) Whole-cell extracts prepared from cells were subjected to SDS-PAGE, followed by immunoblotting using antibodies against cell cycle indicators, and β-actin as the loading control.

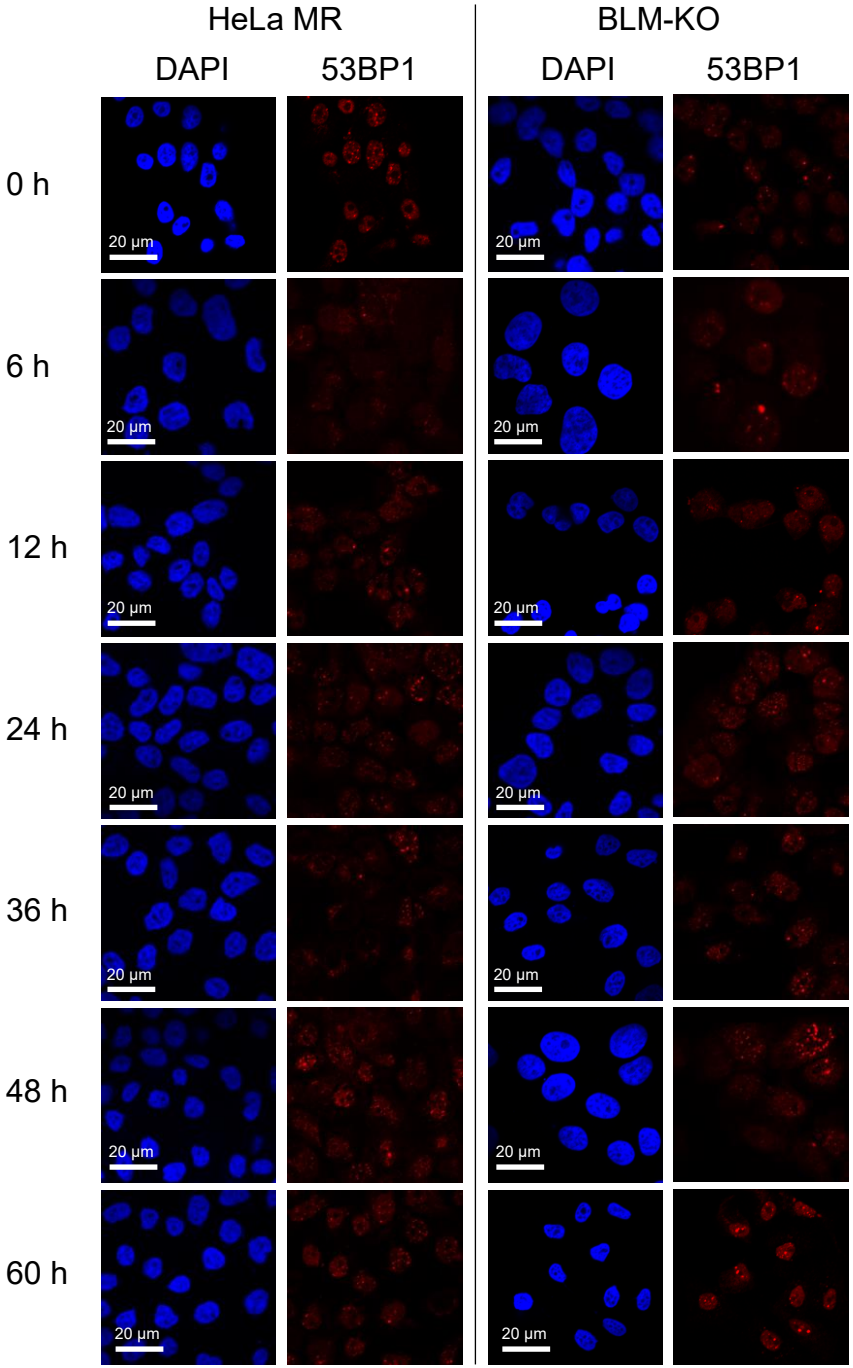

Figure S2. Accumulation of 53BP1 foci in BLM-KO cells after MNU treatment. Synchronized HeLa MR and BLM-KO cells were treated with MNU and immunostained with anti-53BP1 antibody at the indicated times after MNU treatment.

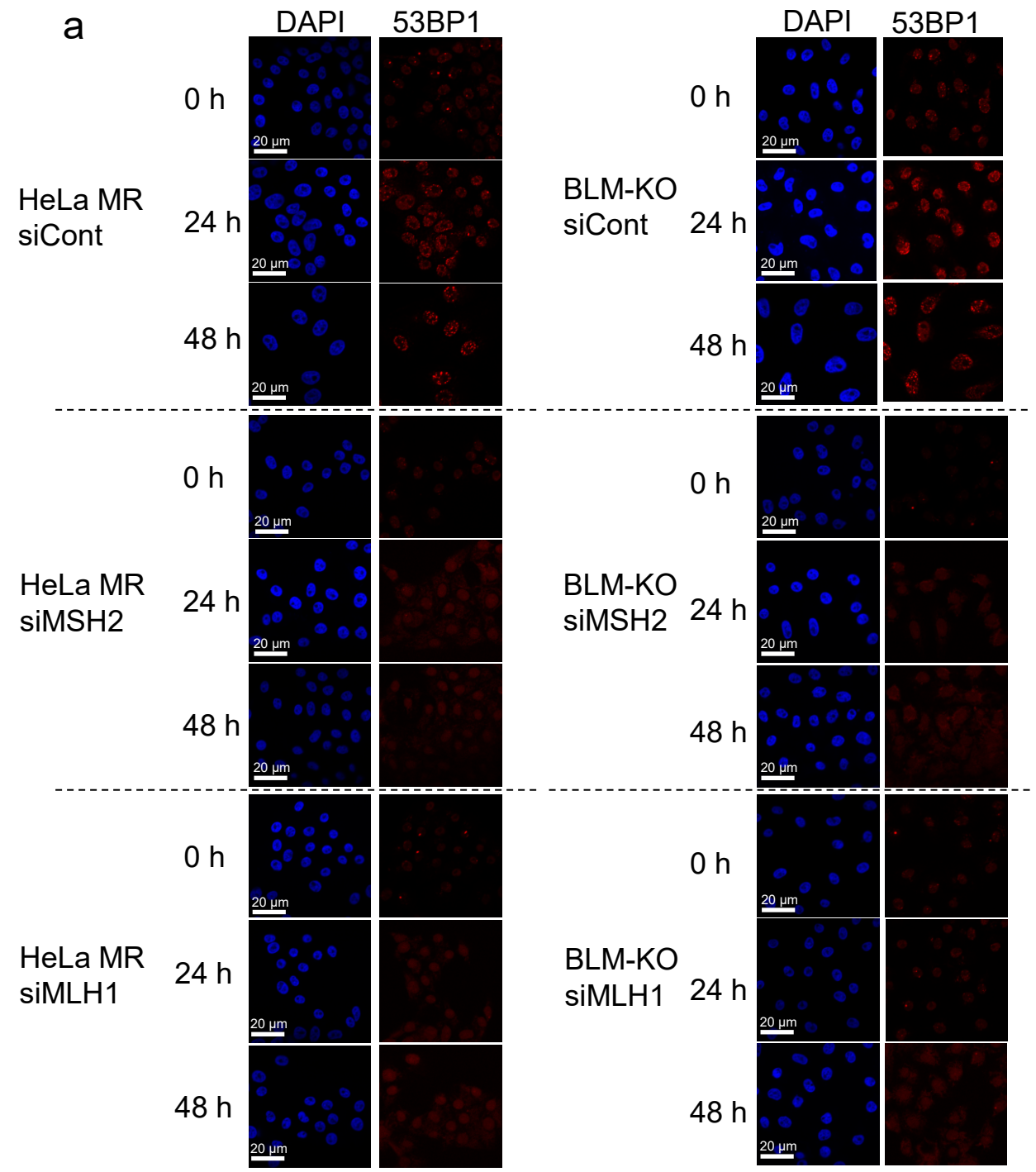

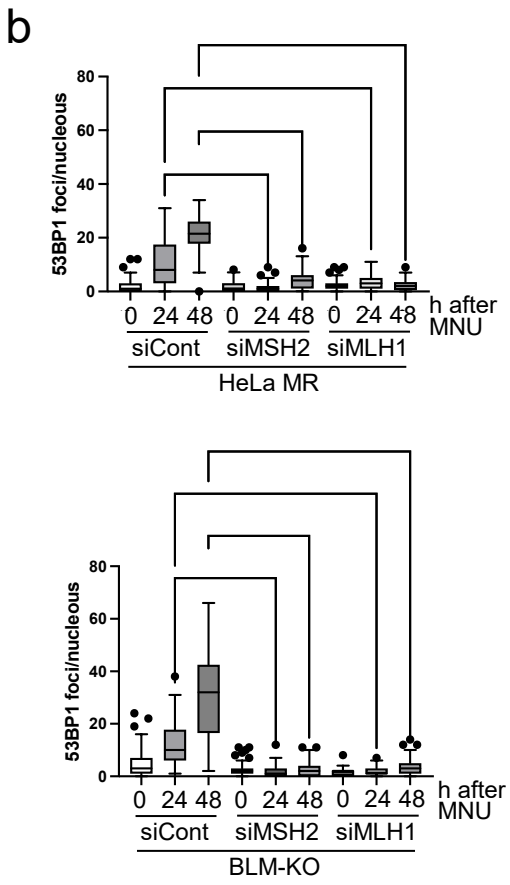

Figure S3. Increased 53BP1 foci in BLM-KO cells after MNU is suppressed by knockdown of MMR genes. siRNA introduced cells were treated with or without MNU, and then immunostained with anti-53BP1 antibody. (a) Representative picture of the immunostaining. (b) The number of nuclear foci of 53BP1 were counted and plotted. ****: p<0.001